Applied Catalysis B: Environmental 205 (2017) 514–518

Contents lists available at ScienceDirect

Applied Catalysis B: Environmental

journal homepage: www.elsevier.com/locate/apcatb

Novel photocatalytic material of organic p–n bilayer responsive to near-infrared energy

Daiki Mendori[a], Takatoshi Hiroya[a], Megumi Ueda[a], Masachika Sanyoushi[a], Keiji Nagai[b], Toshiyuki Abe[a,*]

[a] Department of Frontier Materials Chemistry, Graduate School of Science and Technology, Hirosaki University, 3 Bunkyo-cho, Hirosaki 036-8561, Japan
[b] Laboratory for Chemistry and Life Science, Institute of Innovative Research, Tokyo Institute of Technology, Suzukake-dai, Midori-ku, Yokohama 226-8503, Japan

ARTICLE INFO

Article history:
Received 5 October 2016
Received in revised form
28 December 2016
Accepted 30 December 2016
Available online 31 December 2016

Keywords:
Organic p–n bilayer
Near-infrared
n-Type perylene derivative
p-Type lead phthalocyanine
Photocatalyst

ABSTRACT

An organic p–n bilayer, comprising of an n-type perylene derivative (PTCBI) and p-type lead phthalocyanine (PbPc), was prepared and examined in terms of photoelectrode in the water phase. The PTCBI/PbPc bilayer functioned as a photoanode, which generated a photocurrent due to the oxidation of reactant (i.e., $Fe^{II}(CN)_6^{4-}$) at the PbPc surface. Furthermore, the organo-bilayer also induced a photocatalytic reaction that originated from the oxidising and reducing powers produced at the PbPc and PTCBI, respectively. Based on the photoelectrochemical and photocatalytic studies, it has been noted that the PTCBI/PbPc bilayer can respond to the wide spectrum of solar energy (i.e., 400–1100 nm). However, on using metal-free phthalocyanine (H_2Pc, p-type) as a reference p-type layer and its application as a photocatalyst material in combination with PTCBI, the generated PTCBI/H_2Pc bilayer did not show any photocatalysis particularly under the control irradiation of 700–1200 nm. Thus, the present work demonstrated that the utilisation of a photocatalytic material responding to near-infrared energy is effective towards efficient output into product.

© 2017 Elsevier B.V. All rights reserved.

1. Introduction

Photocatalysts are used for both down-hill ($\Delta G^\circ < 0$, cf. decomposition of pollutant substances) and up-hill reactions ($\Delta G^\circ > 0$, cf. water splitting) [1–10]. TiO_2 are recognised as one of the most active photocatalysts [11–14], which currently leads to its practical uses on the basis of the former reaction; on the other hand, due to its UV response, TiO_2 has been realised to be only effective for the degradation of reactant under outdoor and living-lighting conditions. Therefore, active photocatalyst materials must be developed particularly for the decomposition of a large quantity of reactants into the product, where the application of a wide range of solar spectrum needs to be considered. In conventional instances, band-engineered inorganic semiconductors have been fabricated and used as photocatalysts [15–17]. However, although such photocatalysts can show visible (VIS)-light response, those bring about the lowering of the oxidising and/or reducing power due to the band-gap reduction. Thus, a novel approach for photocatalyst fabrication needs to be suggested to meet the objective mentioned above.

Organic p–n bilayer (including p–n composite in the form of particles) have been studied in terms of both photoelectrodes and photocatalysts in the water phase [18–29]. For instances, when an organo-bilayer, comprising of 3,4,9,10-perylenetetracarboxylic-bis-benzimidazole (PTCBI, n-type) and metal-free phthalocyanine (H_2Pc, p-type), was applied for the degradation of a model substance of pollutant, trimethylamine (TMA), photocatalytic mineralisation of TMA by the PTCBI/H_2Pc bilayer successfully occurred [21,22]. This can be attributed to the photophysical events (such as the formation of exciton by VIS-light absorption of the bilayer, excitation energy transfer of exciton, its charge separation into electrons and holes at the p–n interface, and the following conduction of the carriers through each layer) within the bilayer. This results in the oxidation of TMA at the H_2Pc surface involving O_2 reduction through the reducing power of PTCBI. The most typical characteristics of the organic p–n bilayers of PTCBI are that the entire VIS-light energy was available for both photoelectrode and photocatalytic reactions [18–25], which was distinct from the instances of the conventional inorganic semiconductors.

In the present work, n-type PTCBI was utilised in combination with p-type lead(II) phthalocyanine (PbPc) capable of near-infrared

* Corresponding author.
E-mail address: tabe@hirosaki-u.ac.jp (T. Abe).

http://dx.doi.org/10.1016/j.apcatb.2016.12.071
0926-3373/© 2017 Elsevier B.V. All rights reserved.

(NIR) absorption, aiming at the utilisation of a widespread range of solar spectrum for photoelectrochemical and photocatalytic reactions. In the following sections, detailed results of the PTCBI/PbPc bilayer are discussed and compared with that of a reference bilayer (i.e., PTCBI/H_2Pc) efficient under full VIS-light irradiation.

2. Experimental

PTCBI was synthesised and purified, according to a previously described procedure [30]. The sublimated PbPc grade (Tokyo Kasei Kogyo) was purchased and used as received. H_2Pc (Tokyo Kasei Kogyo) was used as a reference material of p-type organo-semiconductor, which was purified by sublimation at 510 °C prior to the use. The other reagents were of the extra-pure grade. The ITO-coated glass plate (sheet resistance: 8 Ω cm^{-2}; transmittance >85%; ITO thickness: 174 nm) was obtained from Asahi Glass Co., Ltd.

The PTCBI/MPc bilayer (M = Pb or H_2) was prepared by vapour deposition (degree of pressure <1.0×10^{-3} Pa; deposition speed: 0.03 nm s^{-1}), and it comprised of PTCBI coated on an ITO and MPc coated on top of the PTCBI layer (denoted as ITO/PTCBI/MPc). During the vapour deposition, the temperature of the ITO plate was not controlled. Absorption spectral measurements were conducted using a PerkinElmer Lambda 35 spectrophotometer. The resulting absorption spectra of PTCBI [31], PbPc [32], and H_2Pc [31] were identical to those reported earlier, and their absorption coefficients indicated the thickness of the film employed. Since it is considered that the additivity of the absorption coefficients is held in an absorption spectrum of the p–n bilayer, the two unknown parameters, i.e., thicknesses, were estimated by solving simultaneous equations based on absorbance at two distinct wavelengths. Such estimation of film thickness has thus far been conducted dealing with organic p–n bilayers [18–20,23–28].

For measuring cyclic voltammograms, rest potentials, and an action spectrum for photocurrent, a single-compartment cell was employed using a modified ITO working electrode (effective area: 1 cm × 1 cm), a spiral Pt counter electrode, and an Ag/AgCl (in saturated KCl electrolyte) reference electrode. The studies were conducted in an electrolyte solution (pH = 4) within an Ar atmosphere. The photoelectrochemical study was operated using a potentiostat (Hokuto Denko, HA-301) with a function generator (Hokuto Denko, HB-104), a coulomb meter (Hokuto Denko, HF-201), and an X-Y recorder (GRAPHTEC, WX-4000) under illumination. A halogen lamp (light intensity: ca. 100 mW cm^{-2}) was used as the light source under typical conditions (cf. the spectrum of white light employed in the present study was shown in Fig. S1(a)). Particularly when measuring the action spectrum for photocurrent, a halogen lamp was used as the light source in combination with a monochromator (Soma Optics, Ltd., S-10). The light intensity was measured using a power meter (type 3A from Ophir Japan, Ltd.). The incident photon-to-current conversion efficiency (denoted as *IPCE*) was calculated by the following equation:

$$IPCE\ (\%) = ([I/e]/[W/\varepsilon]) \times 100 \quad (1)$$

where, I (A cm^{-2}) is the photocurrent density, e (C) is the elementary electric charge, W (W cm^{-2}) is the light intensity, and ε is the photon energy.

In order to conduct photocatalytic experiments, a twin-compartment cell separated by a salt bridge was employed (*vide infra*). ITO/PTCBI/MPc (oxidation site) and a Pt wire (reduction site) were placed in each compartment and were connected with a lead wire. The photocatalytic study was also carried out under an Ar atmosphere, where ITO/PTCBI/MPc was immersed in an electrolyte solution containing a known concentration of $K_4[Fe^{II}(CN)_6]$ (10 mM, pH = 4) and a Pt wire in an H_3PO_4 solution (pH = 0). For preparing a salt bridge, agar (1.3 g) and KNO_3 (4.74 g) were first dissolved in hot water (1.0×10^{-2} dm^3), and then, the mixture was allowed to flow into the bridging part of the cell and solidify at room temperature. In photocatalytic studies, irradiation of a solar simulator (Asahi Spectra, HAL-C100) was conducted with a band-pass filter (i.e., RT830). The RT830 filter was utilised for control irradiation where photoenergy can be transmitted only from 700 nm to 1200 nm. Spectrum of light irradiated from a solar simulator and transmittance spectrum of the RT830 filter were shown in Fig. S1(b) [33] and (c) [34]. Gaseous product was analysed using a gas chromatograph (GL Sciences, GC-3200) equipped with a thermal conductivity detector and a 5-Å molecular sieve column. Argon was used as the carrier gas.

2.1. Results and discussion

In order to understand the photoelectrode characteristics of ITO/PTCBI/PbPc, cyclic voltammograms were first measured (Fig. 1). As shown in Fig. 1, a photoanodic current was observed due to the oxidation of $Fe^{II}(CN)_6^{4-}$ into $Fe^{III}(CN)_6^{3-}$ at the photoelectrode while in the dark, almost no electrochemical response was observed. The resulting voltammetric characteristics were consistent with previous studies where a photoanodic reaction

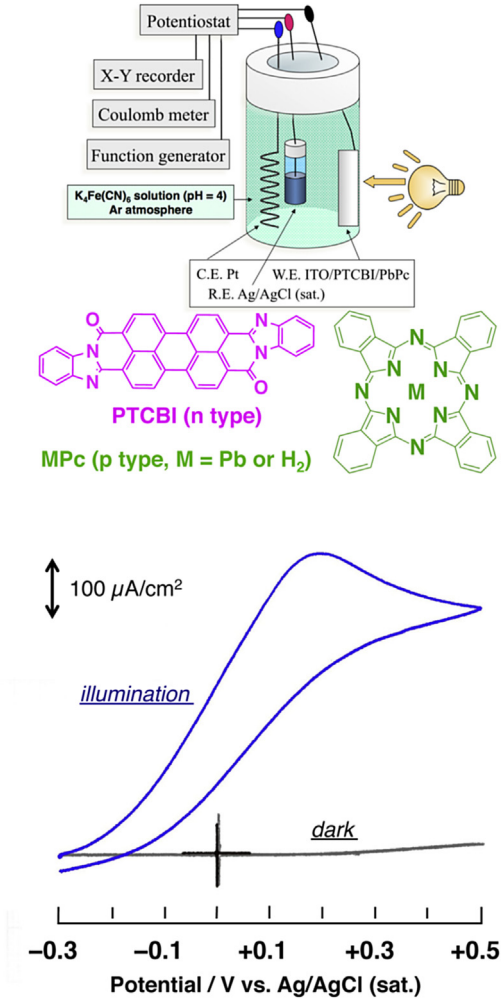

Fig. 1. Cyclic voltammograms (CV) of ITO/PTCBI/PbPc under illumination and in the dark. A schematic illustration of a single-compartment cell employed for CV measurement and the structures of materials employed are also depicted. Film thickness: PTCBI—170 nm, PbPc—85 nm; electrolyte solution, 10 mM $K_4[Fe^{II}(CN)_6]$ (pH = 4); light intensity, ca. 100 mW cm^{-2}; scan rate, 20 mV s^{-1}.

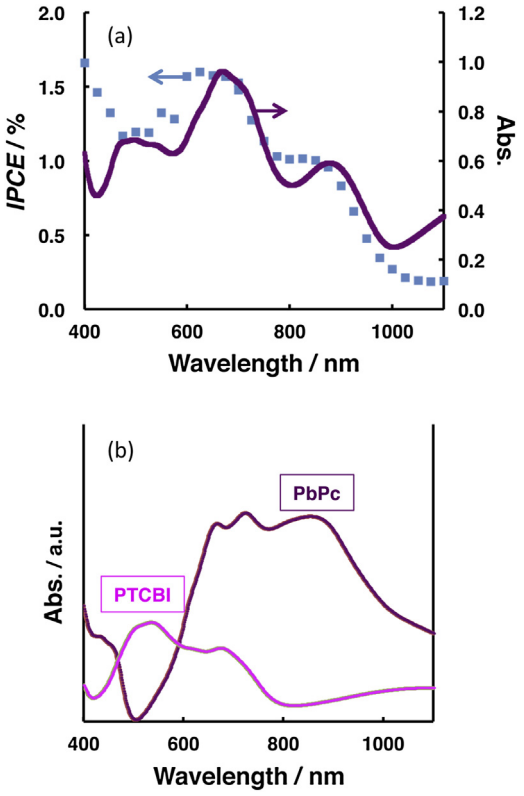

Fig. 2. (a) Action spectrum for photocurrents generated at ITO/PTCBI/PbPc (symbol) and the absorption spectrum of the employed PTCBI/PbPc bilayer (solid line). (b) Absorption spectra of single-layered PTCBI and PbPc. The cell depicted in Fig. 1 was also used for this measurement. Film thickness: PTCBI—160 nm, PbPc—85 nm; applied potential, +0.3 V vs. Ag/AgCl (sat.); electrolyte solution, 10 mM $K_4[Fe^{II}(CN)_6]$ (pH = 4).

can be induced at p-type semiconductor in organic p–n bilayer [18–20,23–25].

For clarifying the origin of photocurrents occurring at ITO/PTCBI/PbPc, an action spectral measurement was conducted. Fig. 2 shows the resulting action spectrum of ITO/PTCBI/PbPc, compared to the absorption spectra of the employed PTCBI/PbPc bilayer as well as the single-layered PTCBI and PbPc. The photoanode of ITO/PTCBI/PbPc was confirmed to respond to widespread photoenergy in the VIS–NIR regions (i.e., 400–1100 nm), due to the absorption of both PTCBI and PbPc.

It appears that a photoanodic response was observed at around 500 nm where no absorption of PbPc was present. It may mean that such a photocurrent can be generated from the sole absorption of PTCBI, successfully leading to the formation of an exciton and the following event of charge separation into electrons and holes occurred at the PTCBI/PbPc interface. This can also be supported by the previous evidence that the quantitative quenching of photoluminescence of PTCBI occurred in the presence of a p-type phthalocyanine layer, indicating that the carrier formation is only possible by PTCBI absorption [35]. Furthermore, the absorption of PbPc also seemed to be responsible for the photoanodic response particularly in the NIR region where an intense peak of PbPc was present.

A photoelectrolysis was conducted according to Scheme 1, where a potential of 0 V (vs. Ag/AgCl) was applied to ITO/PTCBI/PbPc under illumination. As a typical result, the photoelectrochemical oxidation of $Fe^{II}(CN)_6^{4-}$ at ITO/PTCBI/PbPc occurred to involve the reduction of H^+ into H_2 at Pt counter (ca. 13 μL/h). Furthermore, a prolonged study was carried out repeatedly using ITO/PTCBI/PbPc as the photoanode. As shown in Fig. 3, the total amount of H_2

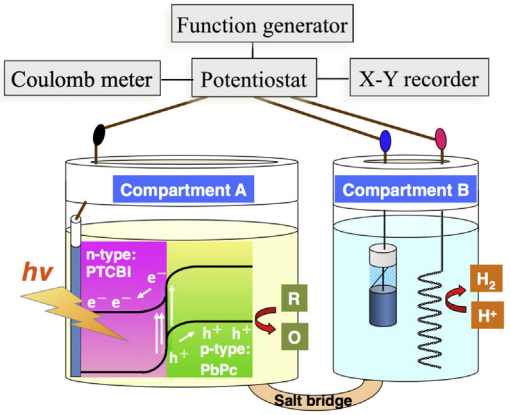

Scheme 1. An illustration of a twin-compartment cell employed for photoelectrolysis experiments.

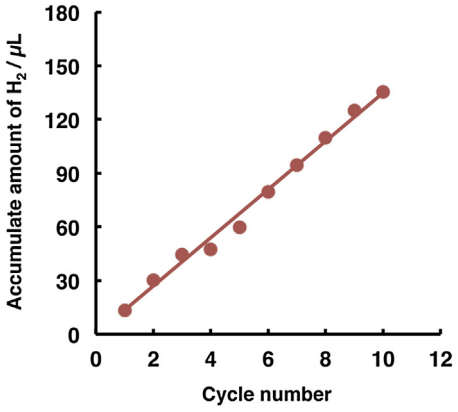

Fig. 3. A long-term photoelectrolysis study of ITO/PTCBI/PbPc. The durable performance of ITO/PTCBI/PbPc was evaluated in terms of the evolved amount of H_2 occurring at Pt counter. After 1h-irradiation (i.e., corresponding to one cycle), the ITO/PTCBI/PbPc photoanode was repeatedly subjected to photoelectrolysis. Film thickness: PTCBI—170 nm, PbPc—90 nm; electrolyte solution: compartment A—1 mM $K_4[Fe(CN)_6]$, compartment B—aqueous H_3PO_4 solution (pH = 0); applied potential, 0 V vs. Ag/AgCl (sat.); light intensity, ca. 70 mW cm^{-2}; irradiation time in one cycle, 1 h.

linearly increased with the cycle number (1 cycle = 1 h), demonstrating its durable performance even after several cycles. The faradaic efficiency for H_2 evolution was estimated according to the conventional method [28], where the resulting value was almost constant (> 80%) in each cycle.

ITO/PTCBI/PbPc was also examined in terms of a photocatalyst material, without applying an electrochemical voltage in the system as depicted in Scheme 1. The typical result has been shown in Table 1, compared to the results of control experiments. In Entry 1, similar to the aforementioned photoelectrochemical result, the $Fe^{II}(CN)_6^{4-}$ oxidation at ITO/PTCBI/PbPc occurred to involve the H_2 evolution at Pt wire while in the absence of PTCBI layer (Entry 2) or PbPc one (Entry 3), no evolution of H_2 was observed to support the effectiveness of the organic p–n bilayer for the photocatalytic reaction. Another control experiment was also conducted (Table 1), where one of the experimental components of Entry 1 was absent (i.e., no addition of electron-donating reagent (Entry 4) or no irradiation to ITO/PTCBI/PbPc (Entry 5)). In Entries 4 and 5, H_2 formation cannot be confirmed; in other words, those results support that the photo-induced oxidation of $Fe^{II}(CN)_6^{4-}$ at ITO/PTCBI/PbPc needs to occur for the evolution of H_2.

We have thus far presented some reports dealing with the PTCBI/H_2Pc bilayer in terms of photoanode and photocatalyst [18,20–23,25]. As shown in Fig. 4, almost no absorption of the

Table 1
Data of photocatalytic H_2 evolution in the system of ITO/PTCBI/PbPc and Pt wire.[a]

Run	H_2 amount/μL	Note
Entry 1	21.2	Full conditions[b]
Entry 2	0	In the absence of PTCBI layer[b]
Entry 3	0	In the absence of PbPc layer[b]
Entry 4	0	In the absence of $Fe^{II}(CN)_6^{4-}$[b,c]
Entry 5	0	Without irradiation[b]

[a] In this experiment, electrochemical apparatuses and Ag/AgCl reference were excluded from the setup depicted in Scheme 1.
[b] Film thickness: PTCBI–180 nm, PbPc–85 nm; effective area (geometrical area) of the photocatalytic device, 1 cm^2; electrolyte solution in compartment A, 10 mM $K_4[Fe^{II}(CN)_6]$ (pH = 4); electrolyte solution in compartment B, H_3PO_4 (pH = 0); light intensity (halogen lamp), ca. 100 mW cm^{-2}; irradiation direction, back side of the ITO-coated face; irradiation time, 1 h.
[c] In compartment A, an aqueous H_3PO_4 solution (pH = 4) was used as electrolyte solution.

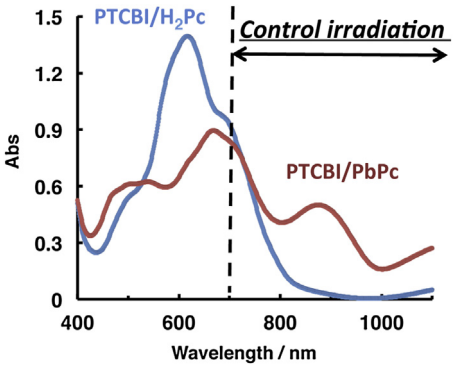

Fig. 4. Absorption spectra of the organo-bilayers employed in the experiments with Table 2. The controlled irradiation range in the corresponding experiments is also shown.

PTCBI/H_2Pc bilayer is present in the NIR region, which is distinct from the PTCBI/PbPc bilayer. Therefore, controlled irradiation was conducted for the photocatalytic system of each bilayer, where only the NIR light (700 ~ 1200 nm) was irradiated through a band-pass filter (RT830). The results are shown in Table 2. H_2 evolution was found to occur only in the case of ITO/PTCBI/PbPc (Entry 1) while no evolution of H_2 can be observed in the system of ITO/PTCBI/H_2Pc (Entry 2), although photocatalytic H_2 evolution was confirmed to occur under the same condition of irradiation as Table 1 (Entry 3). Thus, the results of Tables 1 and 2 demonstrated that the PTCBI/PbPc bilayer is superior to the PTCBI/H_2Pc bilayer in terms of the utilisation of solar energy.

The details of the oxidation of $Fe^{II}(CN)_6^{4-}$ at ITO/PTCBI/PbPc are discussed as follows. We previously reported the photoanodic characteristics of ITO/PTCBI/H_2Pc in the presence of $Fe^{II}(CN)_6^{4-}$ [25], where the $Fe^{II}(CN)_6^{4-}$ oxidation was confirmed to occur at H_2Pc surface. The position of the valence band of PbPc [36], corresponding to oxidising power under illumination (Scheme 1), is consistent with that of H_2Pc [37]. Therefore, $Fe^{II}(CN)_6^{4-}$ oxidation is reasonable to occur in the photoelectrochemical and photocatalytic systems of ITO/PTCBI/PbPc. While the reducing power for photocatalytic H_2 evolution can be generated at the conduction band of PTCBI in an organic p–n bilayer under illumination, as reported by our group [24]. The resulting action spectrum for photocurrents indicated that both the PTCBI and PbPc absorption are responsible for the present photo-induced reaction. Therefore, this can induce the formation of exciton within the PTCBI and PbPc layers. Accordingly, the exciton formed can be separated into electrons and holes at the PTCBI/PbPc interface via excitation energy transfer. In a separate experiment, the magnitude of a built-in potential at the p–n interface was estimated by measuring the rest potential of each single layer, according to the previously reported study procedure [20,38]. The potentials of PTCBI and PbPc were −0.05 V and +0.34 V, respectively. The difference of the resulting values, i.e., ca. 400 mV, exactly corresponds to a built-in potential at the PTCBI/PbPc interface, which can support the mechanism involving charge separation within the employed p–n bilayer. That is, the absorption by the PTCBI/PbPc bilayer triggers a series of photophysical events towards the oxidation of $Fe^{II}(CN)_6^{4-}$, thus resulting in the reduction of H^+ into H_2.

3. Conclusion

This work demonstrates that the PTCBI/PbPc bilayer can function as a photocatalytic material, which can respond to photoenergy in the VIS-NIR region. Such a material can be distinct from conventional photocatalysts of inorganic semiconductors. This refers to the merits possessed by the utilisation of organic p–n bilayer that reacts to a wide spectrum of solar radiation for carrying out the photocatalytic reaction, where oxidising and reducing powers can be produced separately at the p-type and n-type surface, respectively. Those merits are exactly attributed to the employment of the distinct types of organo-semiconductors. When a band-engineered material capable of VIS-light absorption is applied to a photocatalyst, its photocatalytic activity usually decreases with the reduction of band-gap, which involves the decrease in the oxidising/reducing power. The present concept of photocatalysis, featuring both organic semiconductors and p–n bilayers, will be one of the options leading to efficient down-hill and up-hill reactions.

Acknowledgements

This work was partly supported by a grant from the Cooperative Research Program of "Network Joint Research Center for Materials and Devices" (No.20164014 for T.A.) and a Grant-in-Aid for Scientific Research (No.15K05595 for T.A.) from the Ministry of Education, Culture, Sports, Science and Technology, Japan.

Table 2
Data of photocatalytic H_2 evolution under the controlled irradiation.

Run	Oxidation site	Reduction site	H_2 amount/μL	Note
Entry 1	ITO/PTCBI/PbPc [a,b,c]	Pt wire	4.56	–
Entry 2	ITO/PTCBI/H_2Pc [a,b,d]	Pt wire	0	–
Entry 3	ITO/PTCBI/H_2Pc[d,e]	Pt wire	5.43	Experimental conditions were the same as Table 1, except the employment of the PTCBI/H_2Pc bilayer.

[a] These experiments were conducted with the same setup as Table 1, except that only the NIR irradiation was conducted in the range of 700–1200 nm.
[b] electrolyte solution in compartment A, 10 mM $K_4[Fe^{II}(CN)_6]$ (pH = 4); electrolyte solution in compartment B, H_3PO_4 (pH = 0); light intensity (solar simulator), ca. 16 mW cm^{-2}; irradiation direction, back side of the ITO-coated face; irradiation time, 4 h; type of band-pass filter, RT830.
[c] Film thickness: PTCBI—180 nm, PbPc—80 nm; effective area (geometrical area) of the photocatalytic device, 1 cm^2.
[d] Film thickness: PTCBI—185 nm, H_2Pc—70 nm; effective area of the photocatalytic device, 1 cm^2.
[e] Electrolyte solution in compartment A, 10 mM $K_4[Fe^{II}(CN)_6]$ (pH = 4); electrolyte solution in compartment B, H_3PO_4 (pH = 0); use of band-pass filter, no; light intensity (halogen lamp), ca. 100 mW cm^{-2}; irradiation direction, back side of the ITO-coated face; irradiation time, 1 h.

Appendix A. Supplementary data

Supplementary data associated with this article can be found, in the online version, at http://dx.doi.org/10.1016/j.apcatb.2016.12.071.

References

[1] T. Grewe, H. Tüysüz, J. Mater. Chem. A 4 (2016) 3007–3017.
[2] S. Tanigawa, H. Irie, Appl. Catal. B 180 (2016) 1–5.
[3] D. Mateo, I. Esteve-Adell, J. Albero, A. Primo, H. García, Appl. Catal. B 201 (2017) 582–590.
[4] J. Xu, C. Pan, T. Takata, K. Domen, Chem. Commun. 51 (2015) 7191–7194.
[5] T.M. Suzuki, A. Iwase, H. Tanaka, S. Sato, A. Kudo, T. Morikawa, J. Mater. Chem. A 3 (2015) 13283–13290.
[7] K. Iwashina, A. Iwase, Y.H. Ng, R. Amal, A. Kudo, J. Am. Chem. Soc. 137 (2015) 604–607.
[8] W.Y. Lim, M. Hong, G.W. Ho, Dalton Trans. 45 (2016) 552–560.
[9] M. Yan, Y. Wu, F. Zhu, Y. Hua, W. Shi, *2016*, Phys. Chem. Chem. Phys. 18 (*2016*) 3308–3315.
[10] K. Li, Z. Zeng, L. Yan, S. Luo, X. Luo, M. Huo, Y. Guo, Appl. Catal. B 165 (2015) 428–437.
[11] K. Zhang, L. Wang, J.K. Kim, M. Ma, G. Veerappan, C.-L. Lee, Ki-jeong Kong, H. Lee, J.H. Park, Energy Environ. Sci. 9 (2016) 499–503.
[12] A. Morais, C. Longo, J.R. Araujo, M. Barroso, J.R. Durran, A. Flavia Nogueira, *2016*, Phys. Chem. Chem. Phys. 18 (*2016*) 2608–2616.
[13] Y. Dou, S. Zhang, T. Pan, S. Xu, A. Zhou, M. Pu, H. Yan, J. Han, M. Wei, D.G. Evans, X. Duan, Adv. Funct. Mater. 25 (2015) 2243–2249.
[14] H. Li, J. Chen, Z. Xia, J. Xing, J. Mater. Chem. A 3 (2015) 699–705.
[15] K.V. Terebilenko, K.L. Bychkov, V.N. Baumer, N.S. Slobodyanik, M.V. Pavliuk, A. Thapper, I.I. Tokmenko, I.M. Nasieka, V.V. Strelchuk, Dalton Trans. 45 (2016) 3895–3904.
[16] Y. Ham, T. Hisatomi, Y. Goto, Y. Moriya, Y. Sakata, A. Yamakata, J. Kubota, K. Domen, J. Mater. Chem. A 4 (2016) 3027–3033.
[17] G. Li, R. Su, J. Rao, J. Wu, P. Rudolf, G.R. Blake, R.A. de Groot, F. Besenbacher, T.T.M. Palstra, J. Mater. Chem. A 4 (2016) 209–216.
[18] T. Abe, K. Nagai, M. Kaneko, T. Okubo, K. Sekimoto, A. Tajiri, T. Norimatsu, ChemPhysChem 5 (2004) 716–720.
[19] T. Abe, K. Nagai, S. Kabutomori, M. Kaneko, A. Tajiri, T. Norimatsu, Angew. Chem. Int. Ed. 45 (2006) 2778–2781.
[20] T. Abe, S. Miyakushi, K. Nagai, T. Norimatsu, Phys. Chem. Chem. Phys. 10 (2008) 1562–1568.
[21] K. Nagai, T. Abe, Y. Kaneyasu, Y. Yasuda, I. Kimishima, T. Iyoda, H. Imaya, ChemSusChem 4 (2011) 727–730.
[22] K. Nagai, Y. Yasuda, T. Iyoda, T. Abe, ACS Sustainable Chem. Eng. 1 (2013) 1033–1039.
[23] T. Abe, Y. Tanno, T. Ebina, S. Miyakushi, K. Nagai, ACS Appl. Mater. Interfaces 5 (2013) 1248–1253.
[24] T. Abe, Y. Tanno, N. Taira, K. Nagai, RSC Adv. 5 (2015) 46325–46329.
[25] T. Abe, Y. Kamei, K. Nagai, Solid State Sci. 12 (2010) 1136–1139.
[26] T. Abe, S. Tobinai, N. Taira, J. Chiba, T. Itoh, K. Nagai, J. Phys. Chem. C 115 (2011) 7701–7705.
[27] T. Abe, N. Taira, Y. Tanno, Y. Kikuchi, K. Nagai, Chem. Commun. 50 (2014) 1950–1952.
[28] T. Abe, K. Fukui, Y. Kawai, K. Nagai, H. Kato, Chem. Commun. 52 (2016) 7735–7737.
[29] P. Arunachalam, S. Zhang, T. Abe, M. Komura, T. Iyoda, K. Nagai, Appl. Catal. B 193 (2016) 240–247.
[30] T. Maki, H. Hashimoto, Bull. Chem. Soc. Jpn. 25 (1952) 411–413.
[31] T. Morikawa, C. Adachi, T. Tsutsui, S. Saito, Nippon Kagaku Kaishi (1990) 962–967.
[32] D. Campbell, R.A. Collins, Thin Solid Films 261 (2015) 311–316.
[33] http://www.asahi-spectra.co.jp/kiki/kougen/oyosystem/pdf/hal-c100.pdf.
[34] https.//www.hoyacandeo.co.jp/japanese/products/eo_pdf/RT830.pdf.
[35] K. Nagai, Y. Fujimoto, H. Shiroishi, M. Kaneko, T. Norimatsu, T. Yamanaka, Chem. Lett (2001) 354–355.
[36] J. Dai, X. Jiang, H. Wang, D. Yan, Appl. Phys. Lett. 91 (2007) 253503.
[37] K. Suemori, T. Miyata, M. Yokoyama, M. Hiramoto, Appl. Phys. Lett. 86 (2005) 063509.
[38] T. Oekermann, D. Schlettwein, D. Wöhrle, J. Appl. Electrochem. 27 (1997) 1172–1178.